Glyde Sub Basin, Northern Territory

FALCON® Airborne Gravity Gradiometer and Magnetometer Survey

for

Armour Energy Pty Ltd

Operations and Processing Report

Survey Flown: December 2012 to January 2013

By

FUGRO AIRBORNE SURVEYS Pty Ltd
U3/435 Scarborough Beach Rd
Osborne Park, WA 6017
AUSTRALIA

Job# 2381

TABLE OF CONTENTS

FIGURES

TABLES

1 INTRODUCTION

Fugro Airborne Surveys conducted a high-sensitivity aeromagnetic and **FALCON®** Airborne Gravity Gradiometer (AGG) survey over the Glyde Sub Basin survey area under contract with Armour Energy Pty Ltd.

1.1 Survey Location

The Glyde Sub Basin survey area is centred on longitude 136° 12' E, latitude 16º 45' S (see the location map in *Figure 1*).

The production flights took place during December, 2012 and January, 2103 with the first production flight taking place on December 31st and the final flight taking place on January 5th. To complete the survey area coverage a total of 10 production flights were flown, for a combined total of 4,272 line kilometres of data acquired.

Figure 1: Glyde Sub Basin – *Survey Area Location*

1.2 General Disclaimer

It is Fugro Airborne Surveys' understanding that the data and report provided to the client is to be used for the purpose agreed between the parties. That purpose was a significant factor in determining the scope and level of the Services being offered to the Client. Should the purpose for which the data and report is used change, the data and report may no longer be valid or appropriate and any further use of, or reliance upon, the data and report in those circumstances by the Client without Fugro Airborne Surveys' review and advice shall be at the Client's own and sole risk.

The Services were performed by Fugro Airborne Surveys exclusively for the purposes of the Client. Should the data and report be made available in whole or part to any third party, and such party relies thereon, that party does so wholly at its own and sole risk and Fugro Airborne Surveys disclaims any liability to such party.

Where the Services have involved Fugro Airborne Surveys' use of any information provided by the Client or third parties, upon which Fugro Airborne Surveys was reasonably entitled to rely, then the Services are limited by the accuracy of such information. Fugro Airborne Surveys is not liable for any inaccuracies (including any incompleteness) in the said information, save as otherwise provided in the terms of the contract between the Client and Fugro Airborne Surveys.

2 SUMMARY OF SURVEY PARAMETERS

2.1 Survey Area Specifications

Glyde Sub Basin

Total Kilometres (km)	4,272
Clearance Method	Drape
Nominal Terrain Clearance (m)	80
Traverse Line Direction (deg.)	069 / 249
Traverse Line Spacing (m)	400
Tie Line Direction (deg.)	159 / 339
Tie Line Spacing (m)	4000

The survey block is defined by the coordinates in *Table 1*, in UTM Zone 53S projection, referenced to the WGS84 datum.

Corner Number	Easting	Northing
1	608456	8147185
2	600392	8168300
3	628919	8179193
4	641587	8146020
5	648694	8148734
6	655114	8131921
7	647512	8129017
8	651004	8119872
9	635636	8114003
10	621118	8152020

Table 1: Glyde Sub Basin – *Survey Boundary Coordinates*

2.2 Data Recording

The following parameters were recorded during the course of the survey:

- **FALCON® AGG data:** recorded at different intervals.
- **Airborne total magnetic field:** recorded with a 0.1 s sampling rate.
- **Terrain clearance:** provided by the radar altimeter at intervals of 0.1 s.
- **Airborne GPS positional data** (latitude, longitude, height, time and raw range from each satellite being tracked): recorded at intervals of 1 s.
- **Time markers:** in digital data.
- **Ground total magnetic field:** recorded with a 1 s sampling rate.
- **Ground based GPS positional data** (latitude, longitude, height, time and raw range from each satellite being tracked): recorded at intervals of 1 s.
- **Ground surface below aircraft:** mapped by the laser scanner system, scanning at 20 times per second, recording 276 returns per scan (when within range of the instrument and in the absence of thick vegetation).

2.3 Job Safety Plan, HSE Summary

A Job Safety Plan and Job Safety Analysis was prepared and implemented in accordance with the Fugro Airborne Surveys Occupational Safety and Health Management System.

3 FIELD OPERATIONS

3.1 Operations

The survey was based out of Borroloola, Northern Territory. The survey aircraft was operated from Borroloola airport using aircraft fuel available on site. A temporary office was set up in Borroloola at the Savannah Way Motel where all survey operations were run and the post-flight data verification was performed.

3.2 Base Stations

A dual frequency GPS base station was set up at the Savannah Way Motel in order to correct the raw GPS data collected in the aircraft. A secondary GPS base station was available but was not required.

GPS Base Station

Date:	December 31st 2012
Location:	GPS base
Latitude:	16º 4' 18.24421" S
Longitude:	136º 18' 24.68636" E
Height:	68.810 m ellipsoidal

Magnetometer Base Station (CF1)

Location:	Borroloola Airport
Base:	48080 nT

3.3 Field Personnel

The following technical personnel participated in field operations:

Crew Leader:	S. Rawlings
Pilots:	G Hamilton and T. Masefield
Technicians:	S. Rawlings and M. Owen
Project Manager:	P. Johnson
Final QC and Processing:	A. Carbone and P. Chambers

4 QUALITY CONTROL RESULTS

4.1 Survey acquisition issues

During the course of the survey there were no data quality issues with:

AGG instrumentation
Magnetic and GPS base stations
Airborne magnetometer system
Data acquisition systems
Radar altimeter
Laser scanner

4.2 Flight Path Map

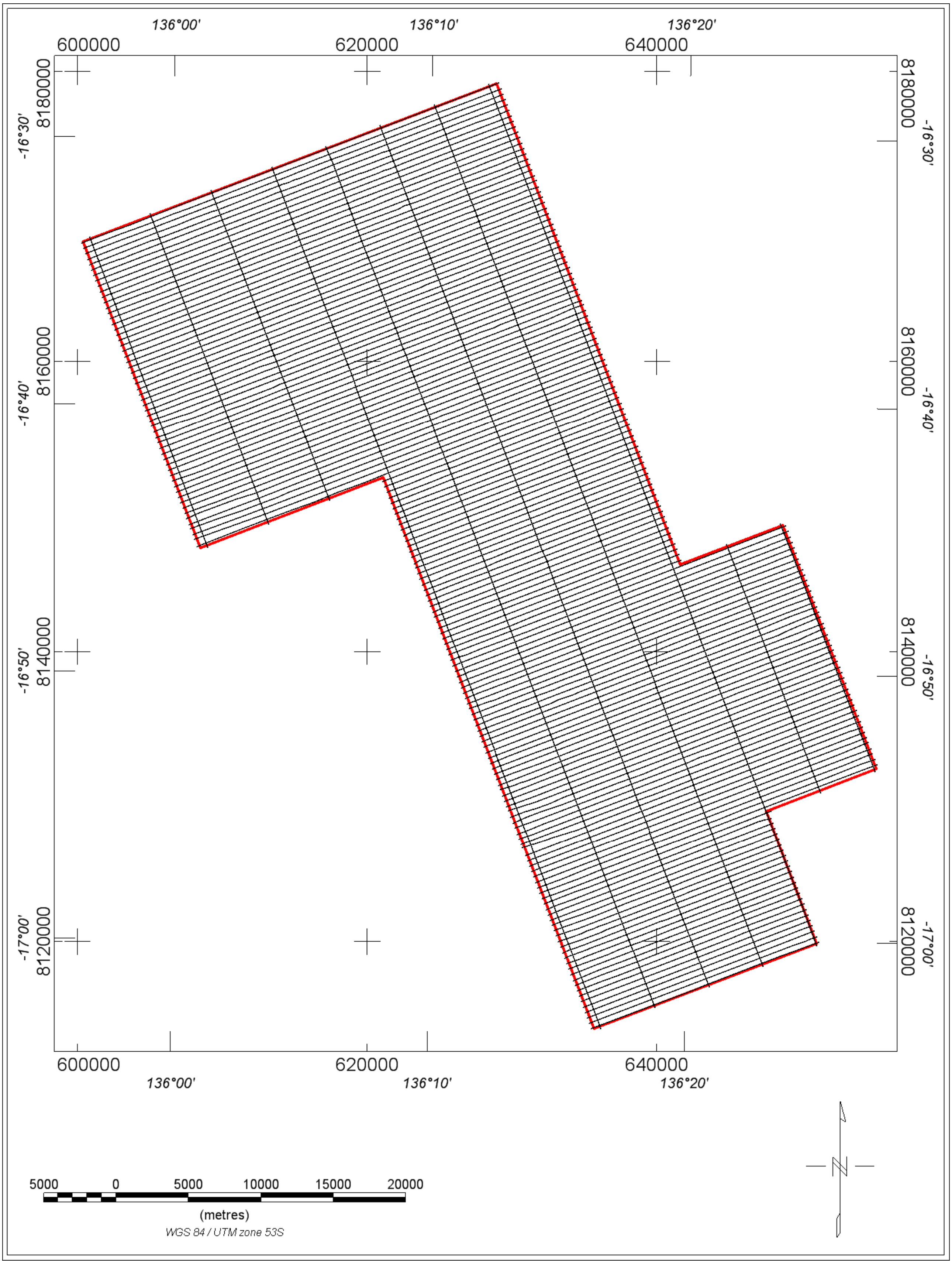

Figure 2: Glyde Sub Basin – *Flight Path map*

4.3 Turbulence

The mean turbulence recorded in the Glyde Sub Basin survey area was 53 milli g (where g = 9.80665 m/sec/sec). Turbulence was variable, ranging from low to high. Primarily it was influenced by the local daily weather patterns, increasing with temperature during the day and decreasing towards late afternoon. The turbulence pattern across the survey area is shown in *Figure 3*.

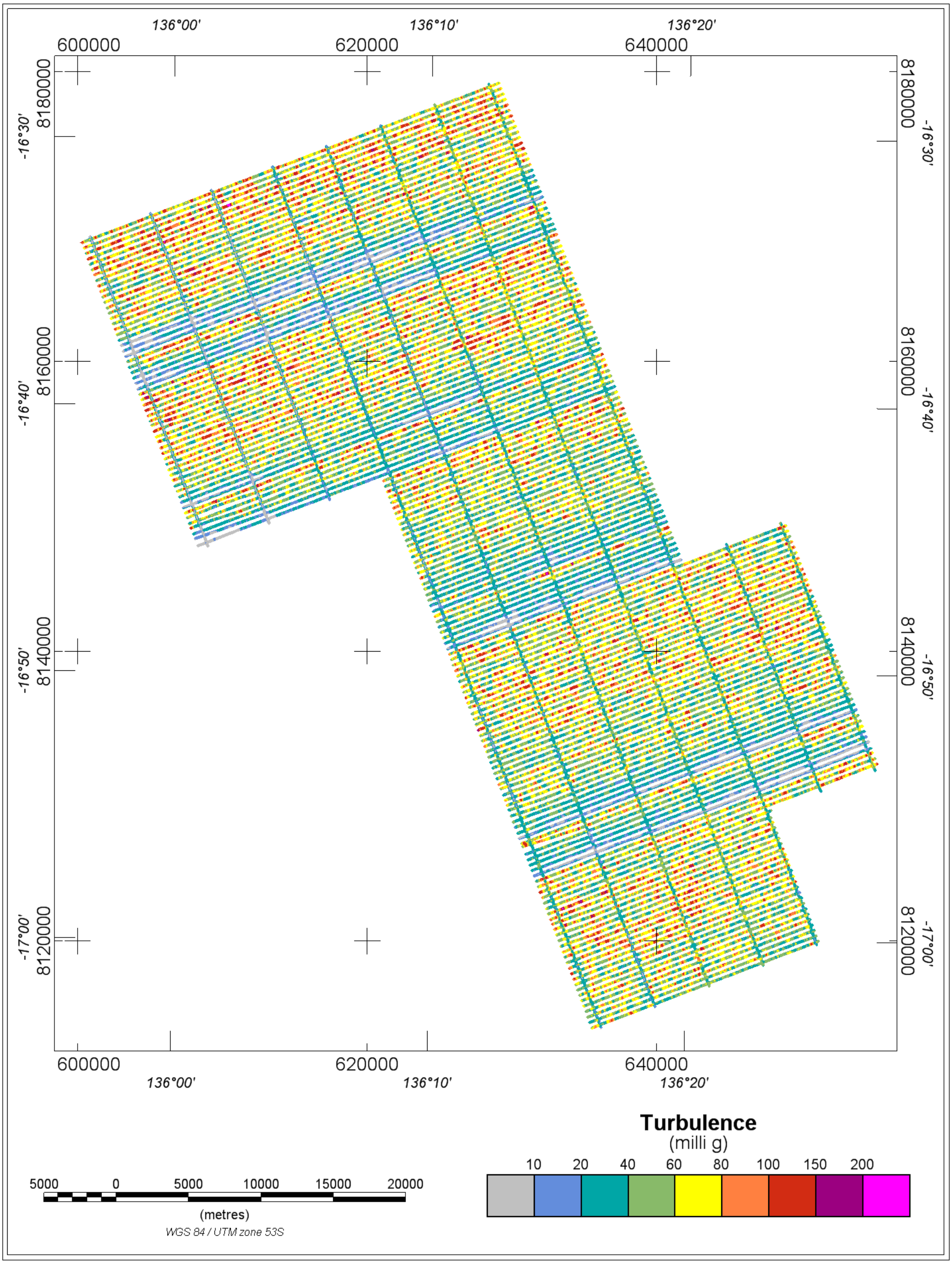

Figure 3: Glyde Sub Basin – *Turbulence (milli g where g = 9.80665 m/sec/sec)*

4.4 AGG System Noise

The system noise is defined to be the standard deviation of half the difference between the A & B complements, for each of the NE and UV curvature components. The results for this survey were very good with values of 1.82 E and 1.80 E for NE and UV respectively.

Figure 4 and *Figure 5* provide a representation of the variation in this standard deviation for each component. This is achieved by gridding a rolling measurement of standard deviation along each line using a window length of 100 data points.

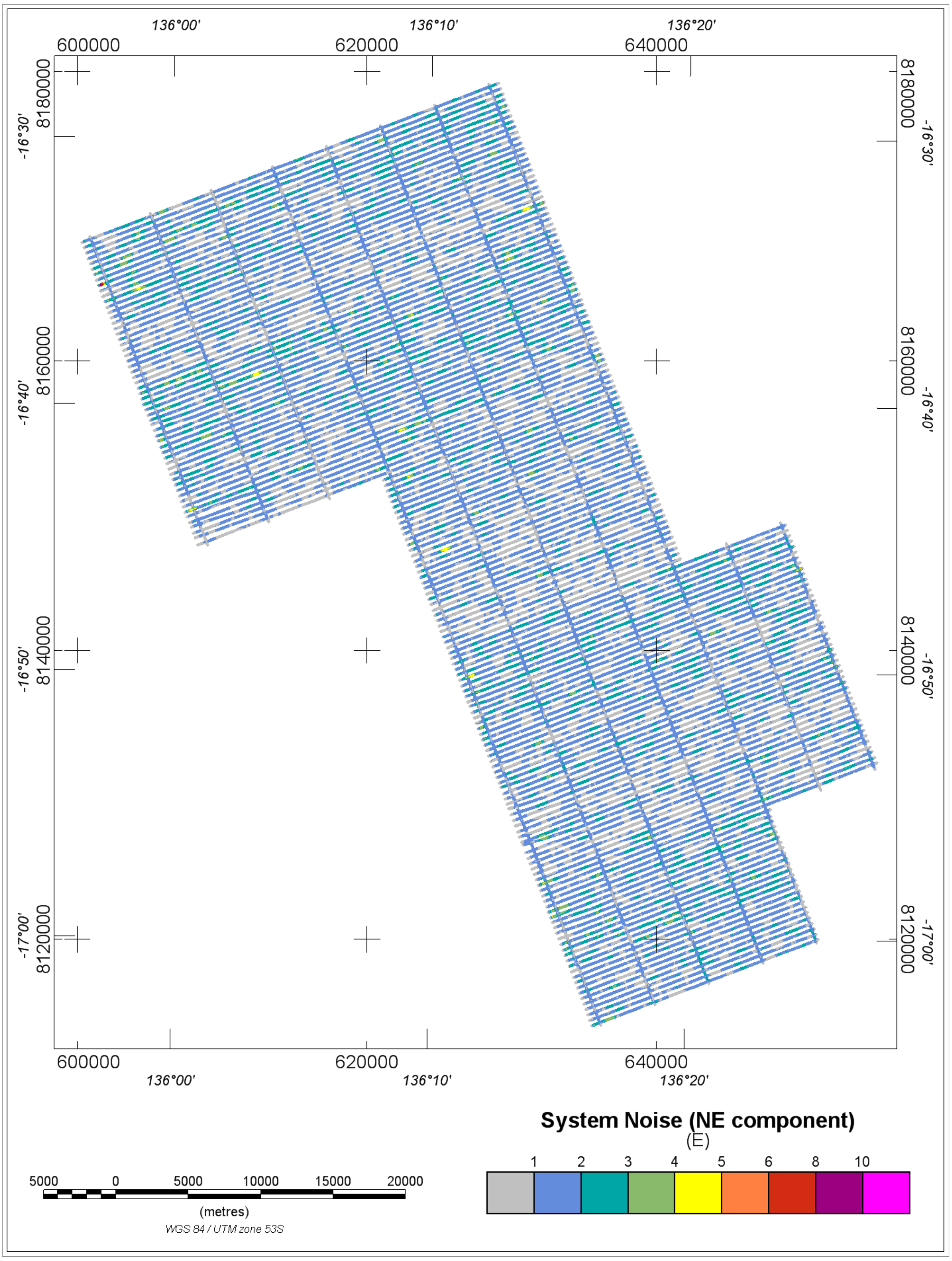

Figure 4: Glyde Sub Basin – *System Noise NE (*E*)*

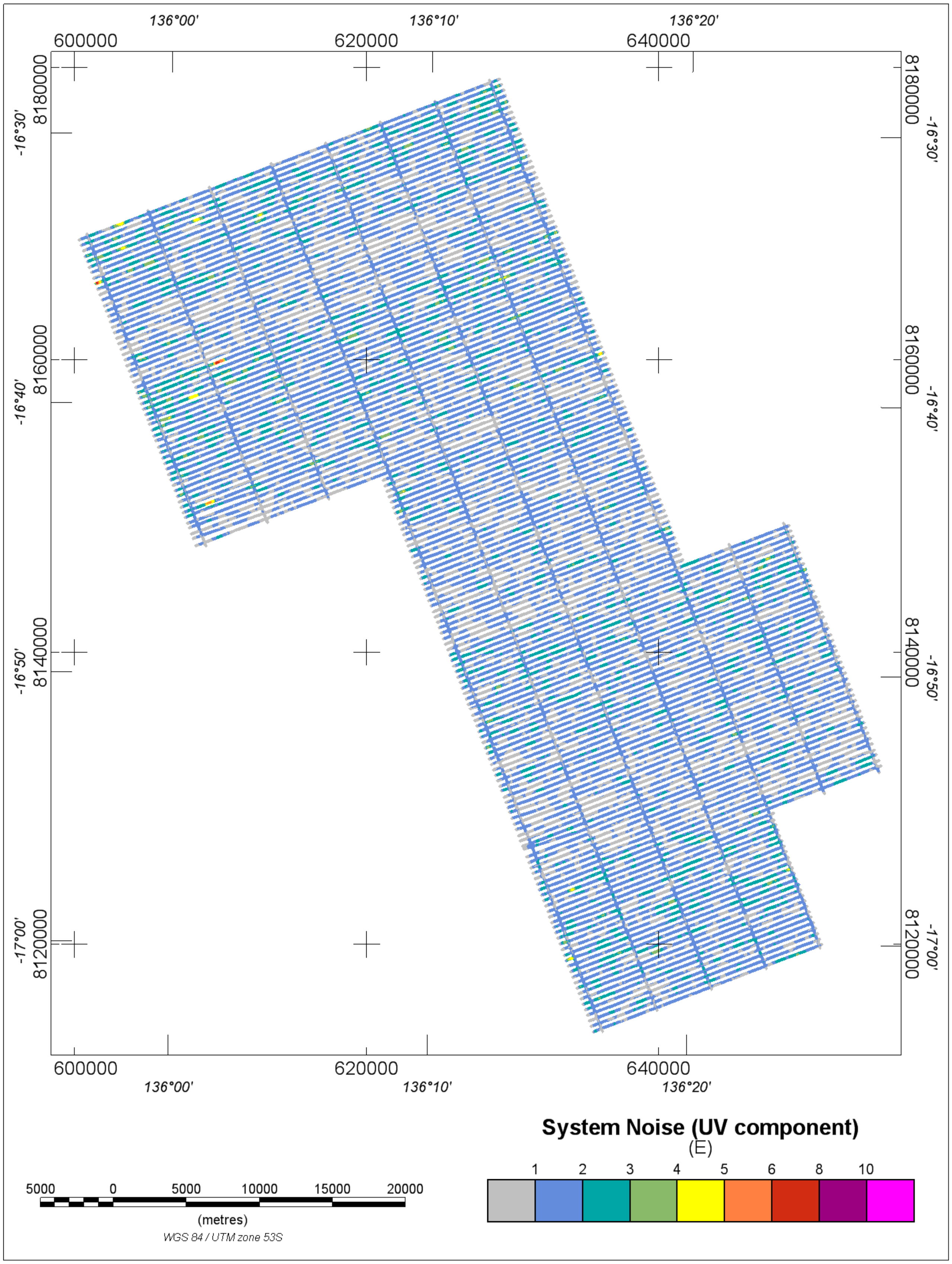

Figure 5: Glyde Sub Basin – *System Noise UV (*E*)*

4.5 Digital Terrain Model

Laser scanner range data were combined with GPS position and height data (adjusted from height above the WGS84 ellipsoid to height above the geoid by applying the Earth Gravitational Model 1996 (EGM96)). The output of this process is a “swath” of terrain elevations extending either side of the aircraft flight path. Width and sample density of this swath varies with aircraft height. Typical values are 100 to 150 metres and 5 to 10 metres respectively.

Because terrain correction of AGG data requires knowledge of the terrain at distances up to at least 10 km from the data location, laser scanner data collected only along the survey line path must be supplemented by data from another source. For this purpose, Shuttle Radar Topography Mission (SRTM) v2 data are usually chosen.

Laser scanner data quality was good with scan density generally above 90%. Laser scanner data were gridded at 20 m with a 1 cell maximum extension beyond data limits. To fill gaps between lines and extend data coverage beyond the survey area, SRTM grid data were excised to an area 15 km beyond the planned survey area. The excised data were adjusted to the level of the laser scanner data using a Fourier domain wrapping method. The two grids were then combined into a single grid such that unmodified laser scanner data were used where defined and adjusted SRTM data were used to fill the gaps and extend the area.

Figure 6 shows the final Digital Terrain Model for the survey area.

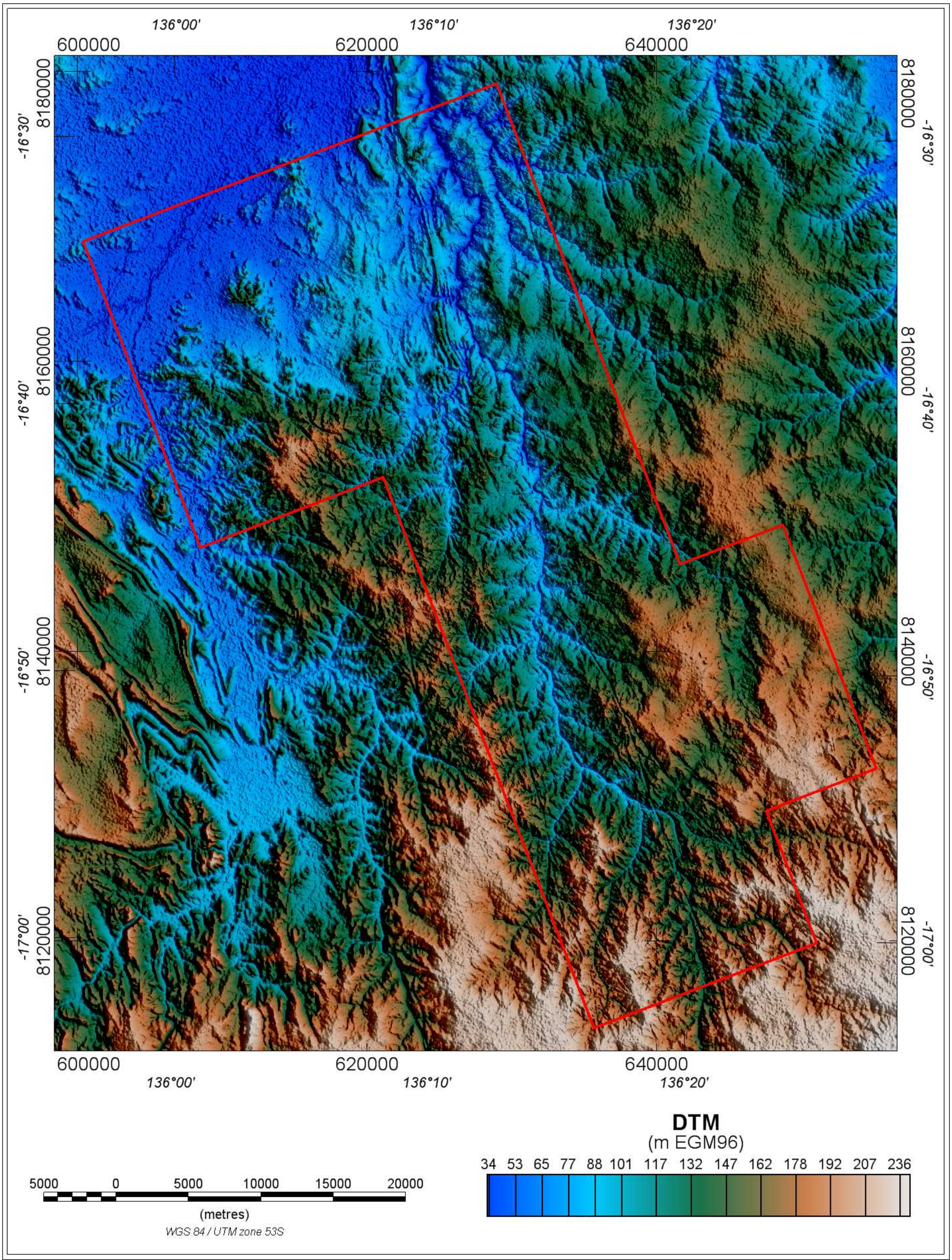

Figure 6: Glyde Sub Basin – *Final Digital Terrain Model (metres, referenced to the EGM96 geoid)*

4.6 Terrain Clearance

Terrain clearance for the Glyde Sub Basin survey averaged slightly above the nominal clearance of 80 m having a mean value of 83 m across the survey area. The terrain clearance, as derived from laser scanner data, is shown in *Figure 7*.

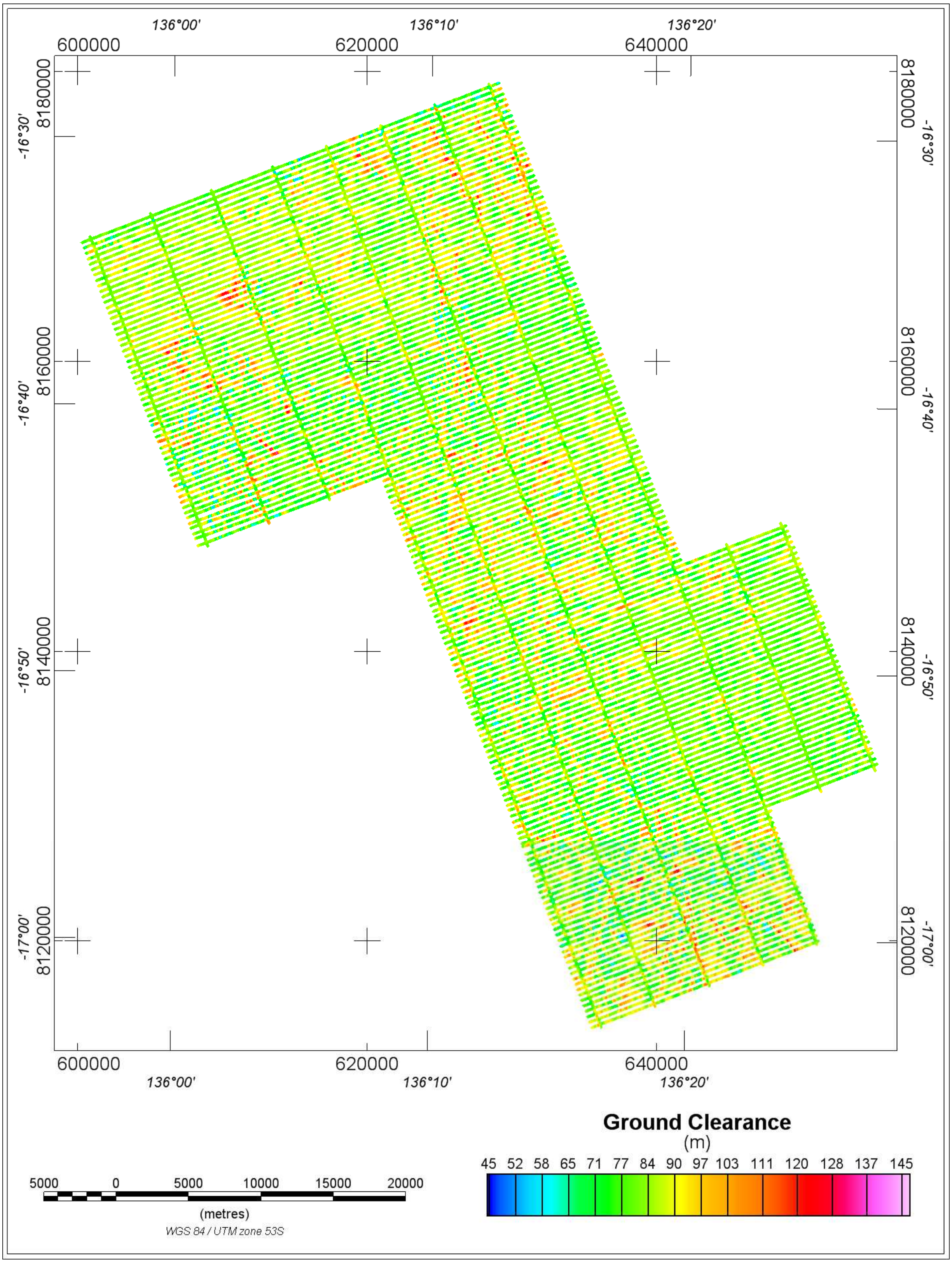

Figure 7: Glyde Sub Basin – *Terrain clearance derived from laser scanner data (metres above ground surface)*

5 FALCON® AIRBORNE GRAVITY GRADIENT (AGG) RESULTS

5.1 Processing Summary

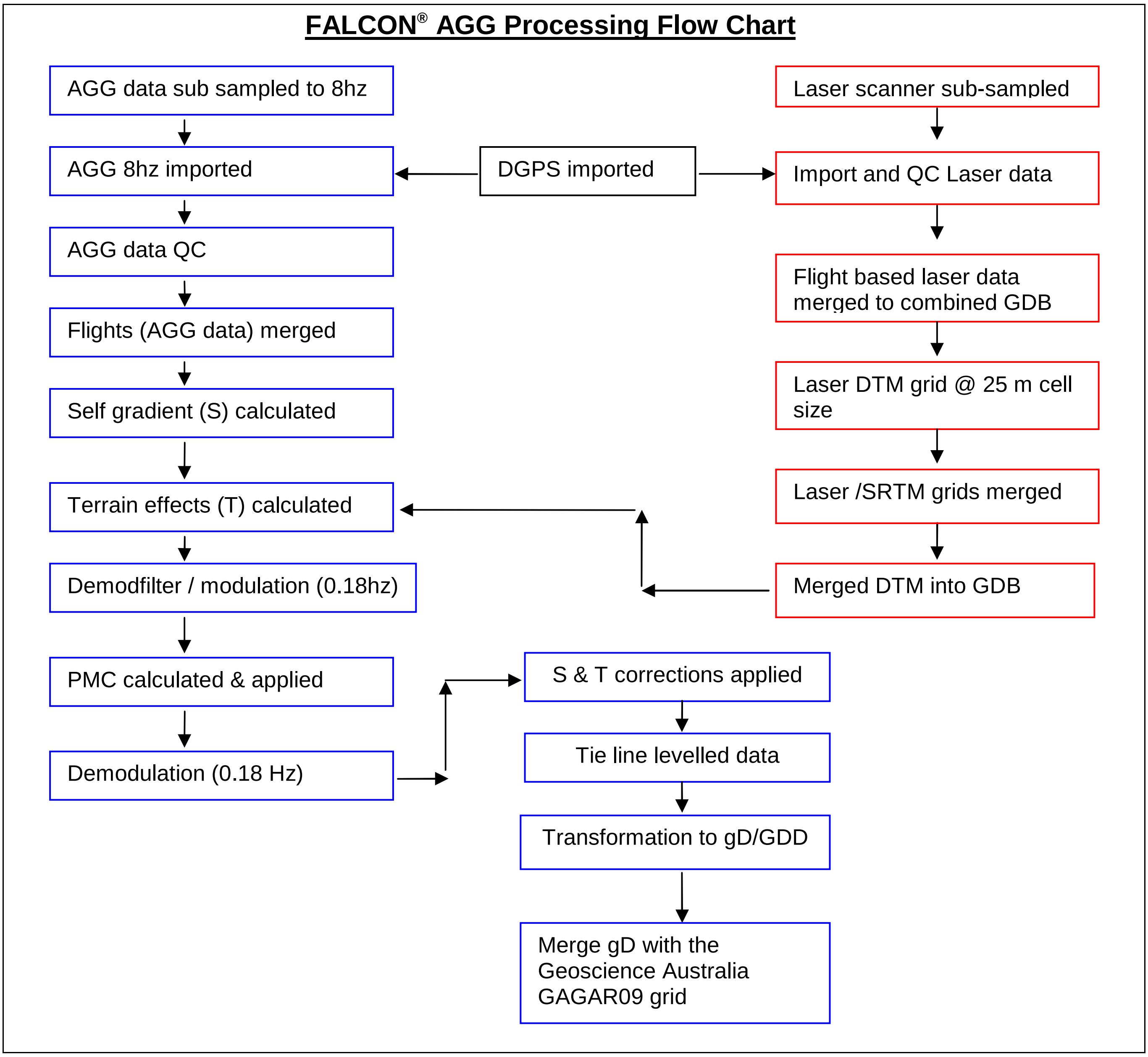

Figure 8: *FALCON®* *AGG Data Processing*

5.2 FALCON® Airborne Gravity Gradiometer Data

Figure 8 summarises the steps involved in processing the AGG data obtained from the survey.

The **FALCON®** Airborne Gravity Gradiometer data were digitally recorded by the ADAS on removable hard drives. The raw data were then copied on to the field processing laptop, backed up twice onto DVD+R media and shipped to Fugro Perth using a secure courier service.

Preliminary processing and QC of the **FALCON®** AGG data were completed on-site using Fugro's DiAGG software.

Further QC and final **FALCON®** AGG data processing were performed by the office-based data processor.

5.3 Radar Altimeter Data

The terrain clearance measured by the radar altimeter in metres was recorded at 10 Hz. The data were plotted and inspected for quality.

5.4 Laser Scanner Data

Laser scanner returns were recorded at a rate of 20 scans per second with each scan returning 276 data points. Each return was converted to ground surface elevation by combining scanner range and angle data with aircraft position and attitude data. Computed elevations were then sub sampled by first dividing each scan into ten segments and combining five adjacent scans per segment , then using a special algorithm to select the optimum return within each data "bin" thus formed. Sub-sampled laser scanner data were edited to remove spikes prior to gridding.

5.5 Positional Data

A number of programs were executed for the compilation of navigation data in order to reformat and recalculate positions in differential mode. Waypoint's GrafNav GPS processing software was used to calculate DGPS positions from raw range data obtained from the moving (airborne) and stationary (ground) receivers.

The GPS ground station position was determined by logging GPS data continuously for 24 hours prior to survey flights commencing. The GPS data were processed and quality controlled completely in the field using the WGS84 datum.

Parameters for the WGS84 datum are:

Ellipsoid:	WGS84
Semi-major axis:	6378137.0 m
1/flattening:	298.257

All processing was performed using WGS84/UTM Zone 53S coordinates. Final line data and final grid data were supplied in this projection.

5.6 Terrain Correction

Terrain corrections were derived from the digital terrain model grid for every data point in the survey. A terrain density of 1.00 g/cm^3 was used to compute the terrain correction channels, which were then multiplied by the chosen correction density before being subtracted from the data.

In the consultation with the client and after testing with a terrain density tool, the standard correction density of 2.67 g/cm^3 was selected. Typically 2.67 g/cm^3 will work well for most terrain types but may lead to over correction or under correction in some areas.

5.7 Tie line Levelling

The terrain corrected data and the uncorrected data were then tie line levelled. All lines were used in the levelling process to produce a single combined set of levelled data.

WARNING: Since tie line levelling is performed after terrain correction, the use of the levelled uncorrected data together with the terrain correction channels to create data corrected for a different terrain density will almost certainly result in residual levelling errors in the new corrected data. An alternative method for computing terrain corrected data for additional densities is described in section *9.11*.

5.8 Micro-levelling

Micro-levelling was applied to the tie line levelled data to remove residual long wavelength levelling errors.

5.9 FALCON® Airborne Gravity Gradient Data - G_{DD} & g_D

The transformation into G_{DD} and g_D was accomplished using two methods: Fourier domain transformation and the Method of Equivalent Sources

5.9.1 Fourier

The Fourier domain transformation method upward continues data to a horizontal surface on which the transformation is applied. The transformed data are then downward continued to the computation surface.

A low-pass filter is applied to improve the signal to noise ratio by removing artefacts of the continuation process and other information which is known to be beyond the sampling resolution. A cut-off wavelength of 400 m was used in the low-pass filter.

5.9.2 Equivalent Source

The equivalent source transformation utilises a smooth model inversion to calculate the density of a surface of sources followed by a forward calculation to produce g_D and G_{DD}. It was possible to closely match the short to medium wavelength characteristics of the Fourier results by placing the sources at a depth of 400 metres.

5.9.3 Drape Surfaces

Both transformations use a smoothed surface onto which the output data are projected. These surfaces are smoother equivalents of the actual flying surface.

The Fourier and equivalent source (density 2.67 g/cm^3) G_{DD} maps are shown in *Figure 9* and *Figure 10* respectively.

Two versions of vertical gravity (g_D) are presented: Fourier, derived by integrating G_{DD}; and equivalent source, derived directly from the modelled sources. The (density 2.67 g/cm^3) Fourier result is presented in *Figure 11* and the (density 2.67 g/cm^3) equivalent source result is presented in *Figure 12*.

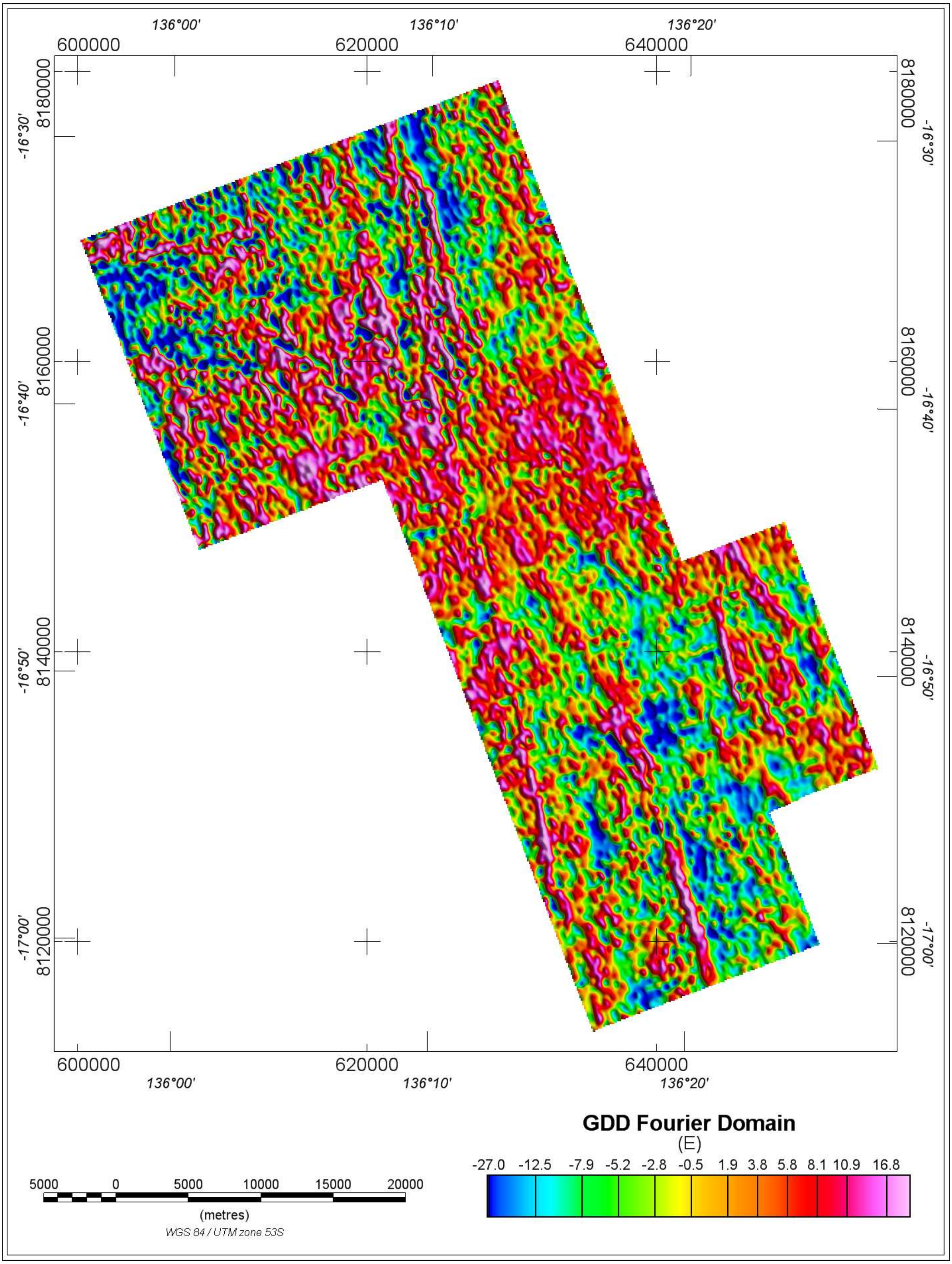

Figure 9: Glyde Sub Basin – *Vertical Gravity Gradient (G_{DD}) from Fourier processing (E).*

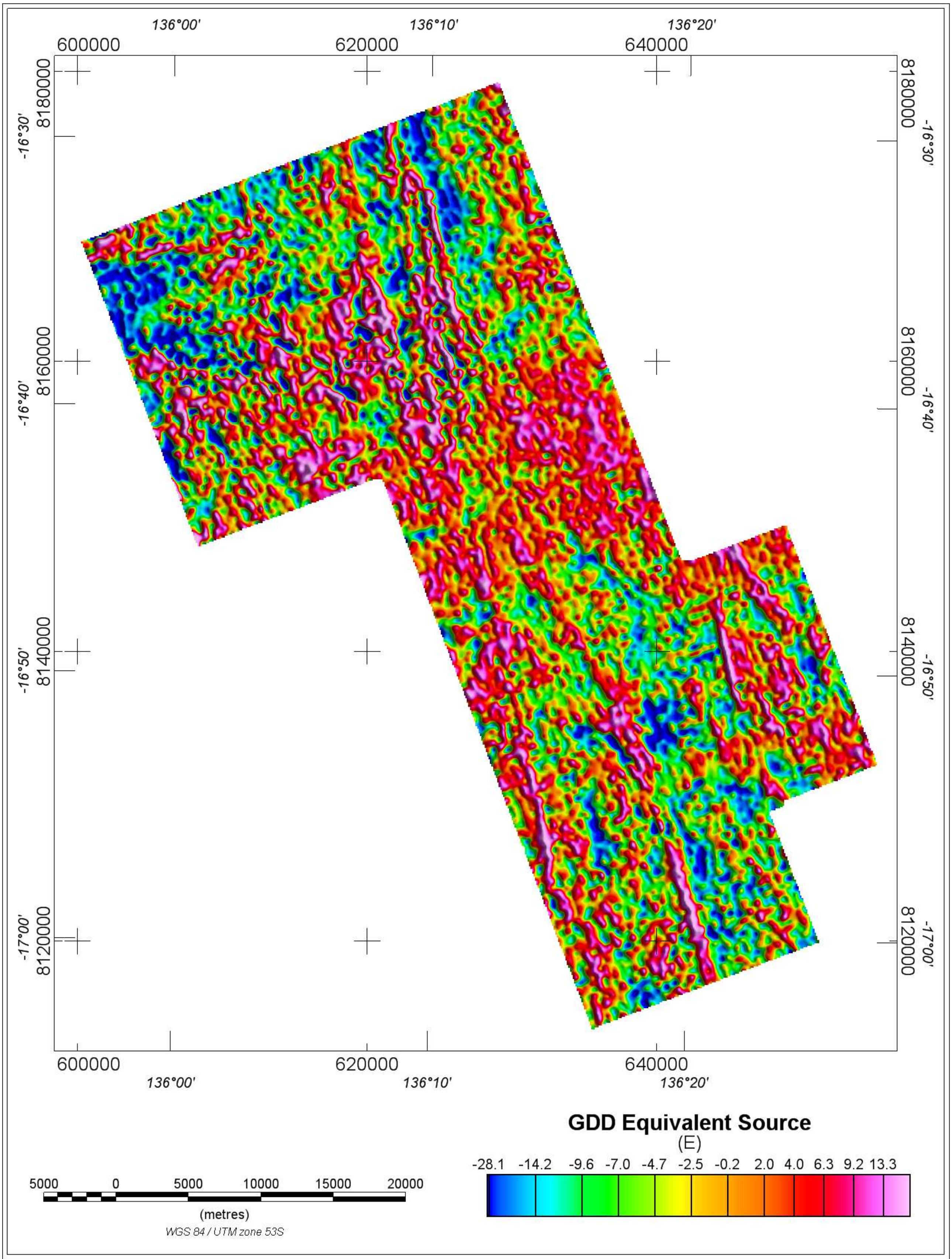

Figure 10: Glyde Sub Basin – *Vertical Gravity Gradient (G_{DD}) from equivalent source processing (E).*

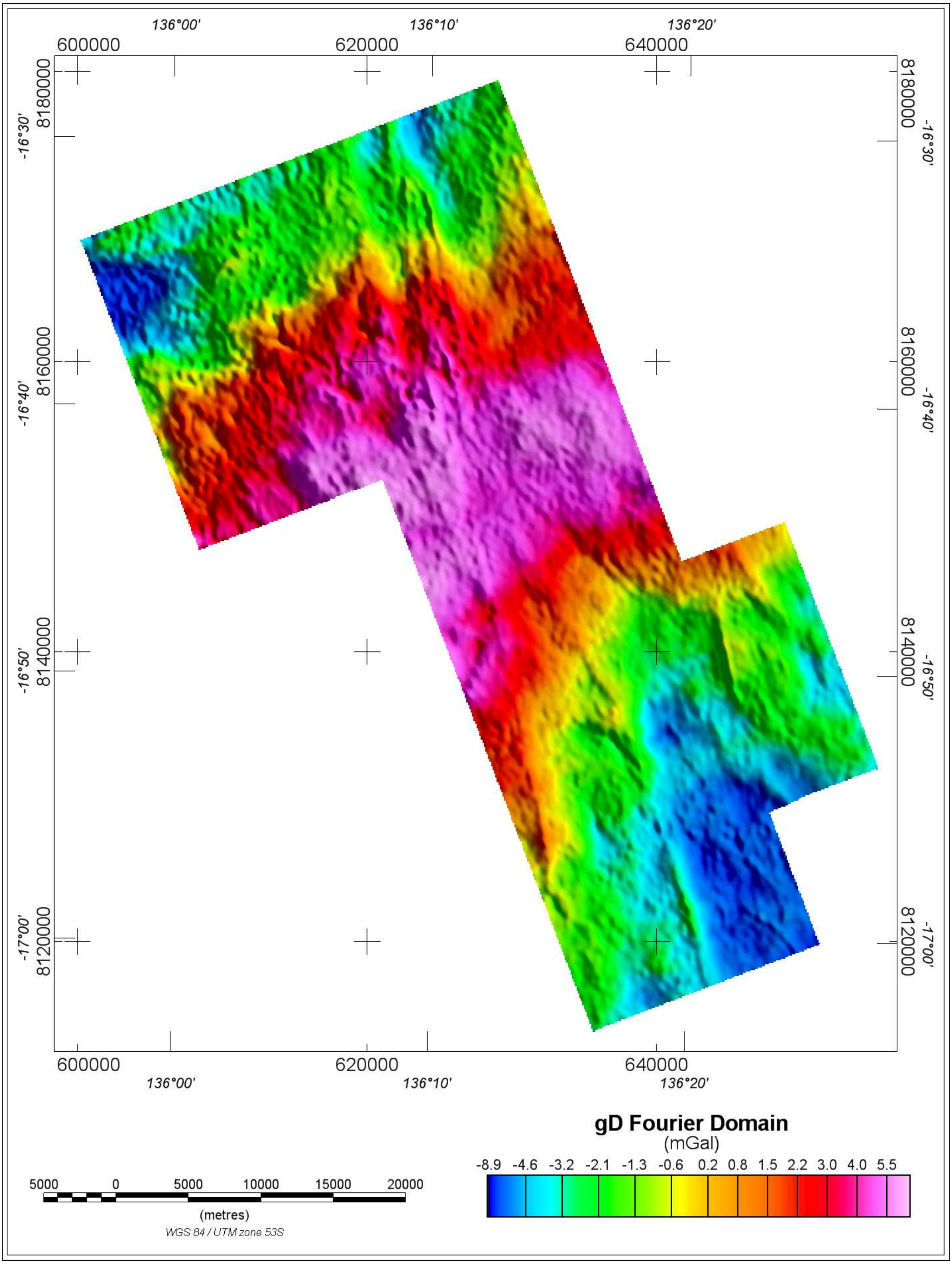

Figure 11: Glyde Sub Basin – *Vertical Gravity (g_D) from Fourier processing (mGal)*

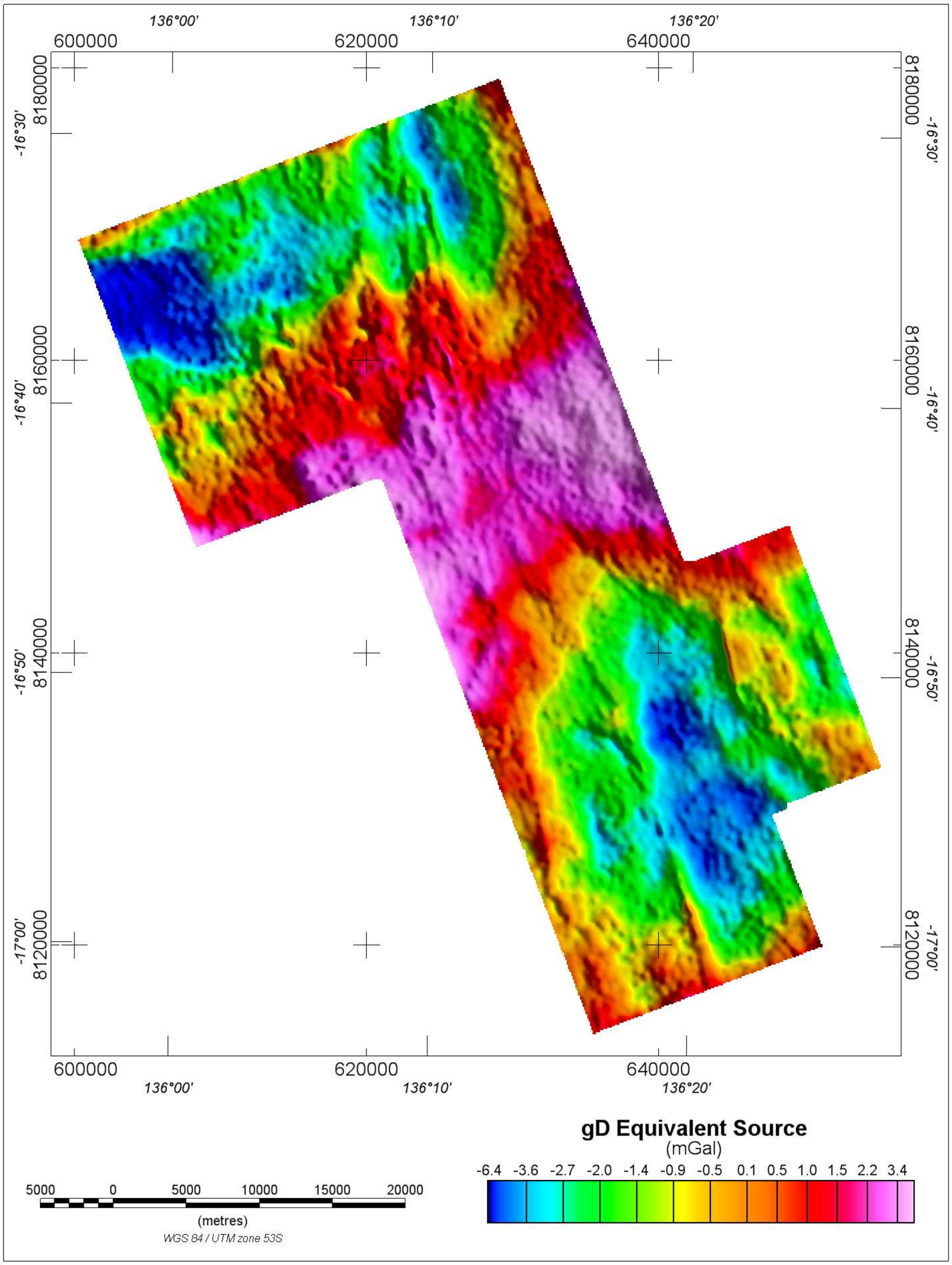

Figure 12: Glyde Sub Basin – *Vertical Gravity (g_D) from equivalent source processing (mGal)*

5.10 Conforming g_D to regional gravity

As discussed in section *9.3*, the long wavelength information in g_D (both the Fourier and equivalent source versions) can be improved by incorporating ancillary information. Such information is available in the form of the Canadian Gravity Anomaly Data Base.

As discussed in section *9.3*, the long wavelength information in g_D (both the Fourier and equivalent source versions) can be improved by incorporating ancillary information. Such information is available in the form of the Geoscience Australia "Gravity Anomaly Grid of the Australian Region (June 2009)" (GAGAR09).

The Fourier and equivalent source g_D grids were conformed to a subset of the GAGAR09 grid as follows. The (density 2.67 g/cm^3) results are presented in *Figure 13* and *Figure 14.*

- Low pass filter the regional data using a cosine squared filter with cut-off at 30 km, tapering to 20 km.
- High pass filter the g_D data (Fourier and equivalent source) using a cosine squared filter with cut-off at 30 km, tapering to 20 km.
- Conform the Fourier and equivalent source data to the regional data by addition of the filtered grids. The filter design is such that this method provides uniform frequency response across the overlap frequencies.

Further discussion of this method can be found in Dransfield (2010).

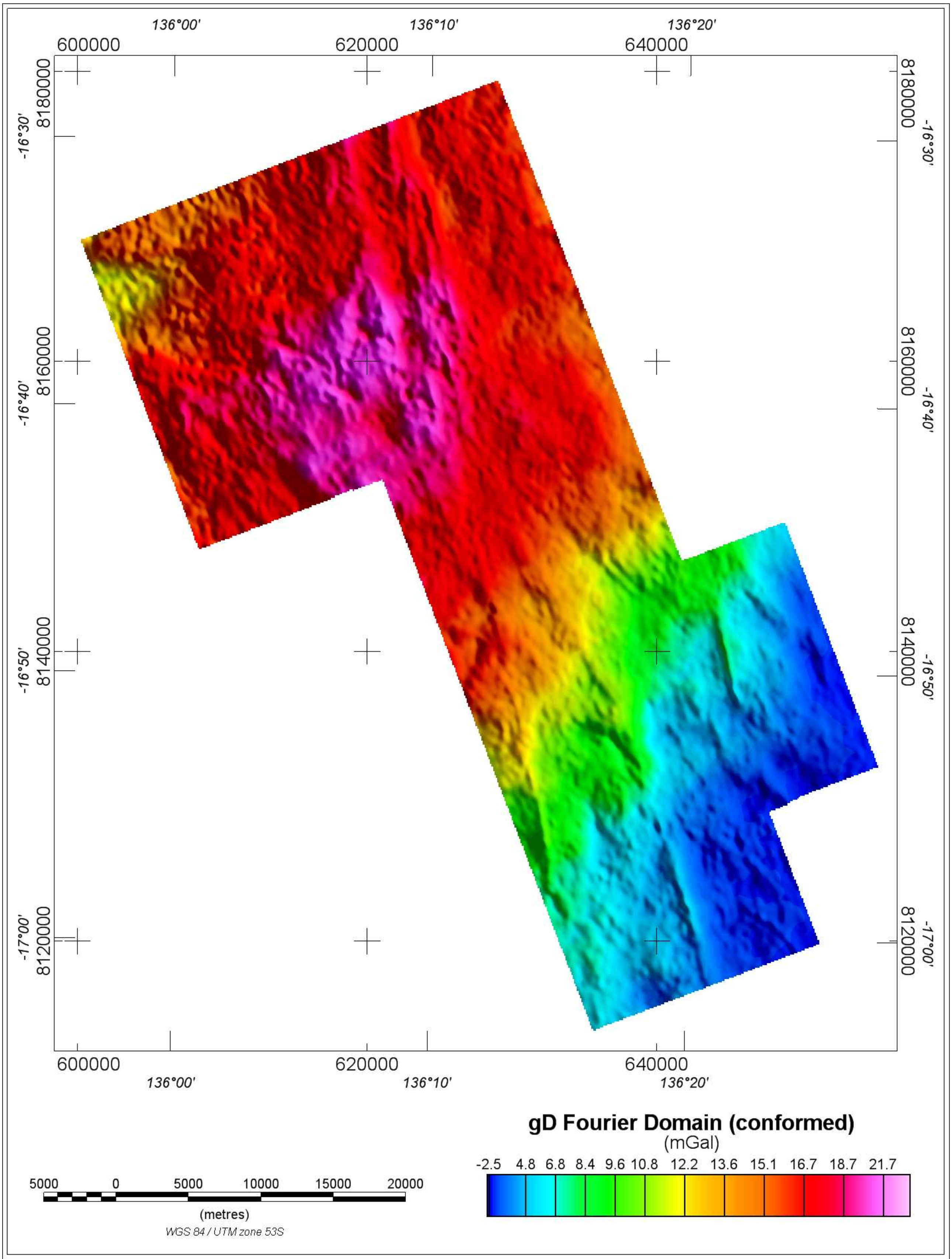

Figure 13: Glyde Sub Basin – *Vertical Gravity (g_D) from Fourier processing conformed to regional gravity data (mGal)*

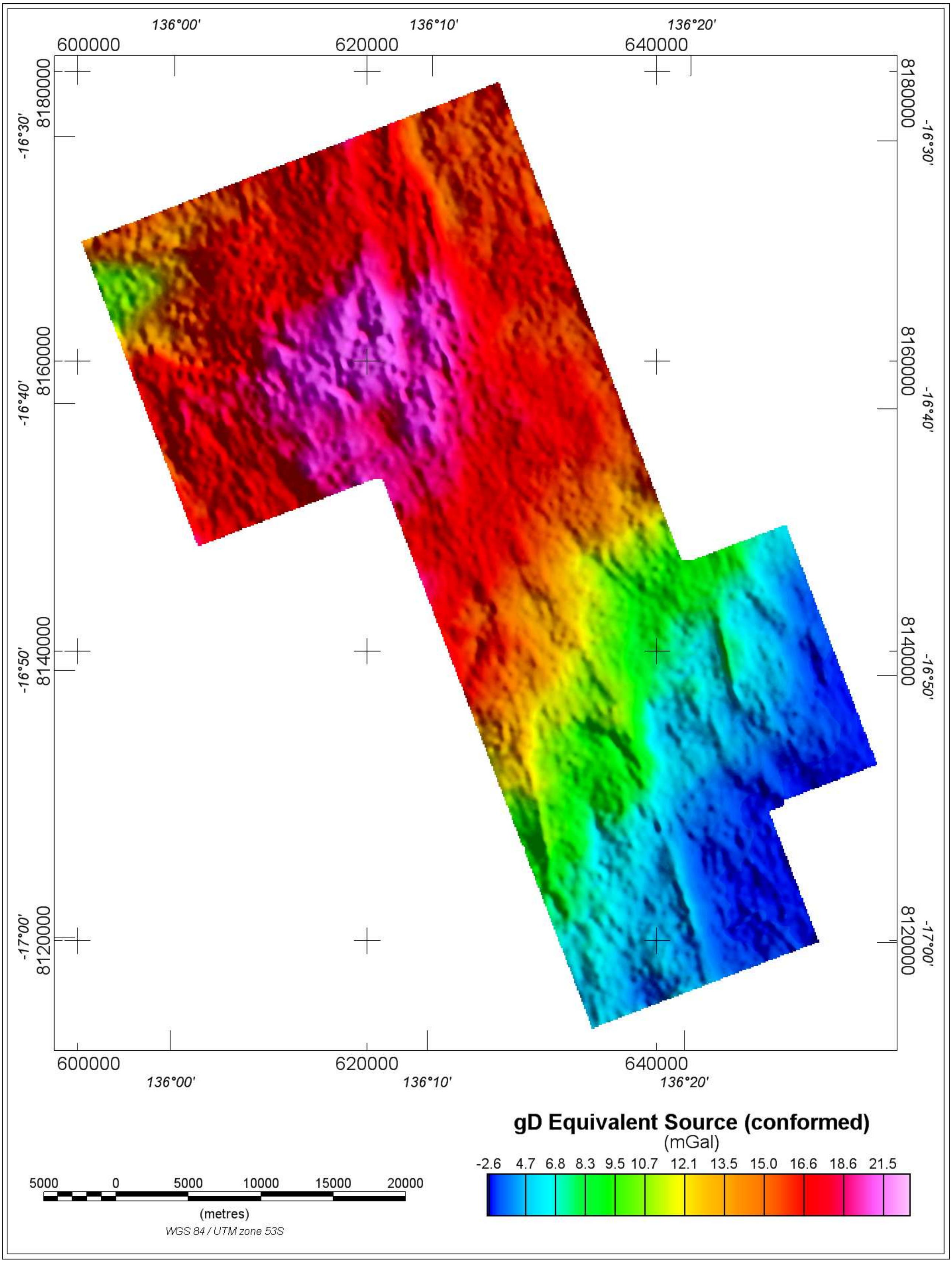

Figure 14: Glyde Sub Basin – *Vertical Gravity (g_D) from equivalent source processing conformed to regional gravity data (mGal).*

6 AEROMAGNETIC RESULTS

6.1 Processing Summary

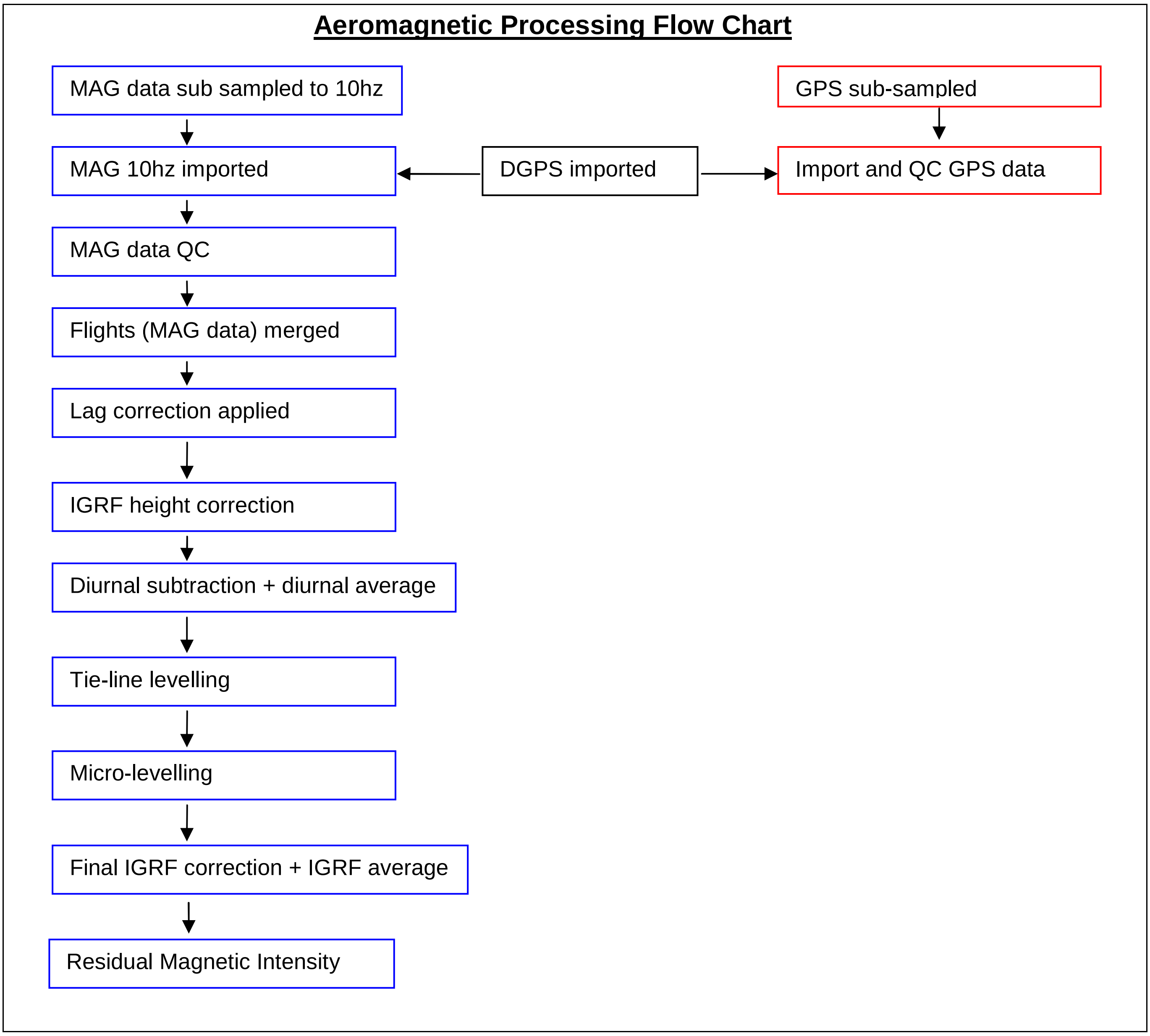

Figure 15: *Aeromagnetic Data Processing*

6.2 Aeromagnetic Data

Figure 15 summarises the steps involved in processing the aeromagnetic data obtained from the survey.

The aeromagnetic data were digitally recorded by the FASDAS on removable hard drives. The raw data were then copied onto the field processing laptop, backed up twice onto hard drive media and sent via FTP to Fugro's secure server.

Preliminary QC of the aeromagnetic data was completed on-site using Fugro's proprietary ATLAS software.

Further QC and aeromagnetic data processing were performed by the office based data processor.

6.3 Radar Altimeter Data

The terrain clearance measured by the radar altimeter in metres was recorded at 10 Hz. The data were plotted and inspected for quality.

6.4 Positional Data

A number of programs were executed for the compilation of navigation data in order to reformat and recalculate positions in differential mode. Waypoint's GrafNav GPS processing software was used to calculate DGPS positions from raw range data obtained from the moving (airborne) and stationary (ground) receivers.

The GPS ground station position was determined by logging GPS data continuously for 24 hours prior to survey flights commencing. The GPS data were processed and quality controlled completely in the field using the WGS84 datum.

Parameters for the WGS84 datum are:

Ellipsoid:	WGS84
Semi-major axis:	6378137.0 m
1/flattening:	298.257

All processing was performed using WGS84/UTM Zone 53S coordinates. Final line and grid data were supplied in this projection.

6.5 Lag Correction

All aeromagnetic data were lagged while importing raw data. Any necessary adjustments are made during final processing and in this case, no further lag correction was applied.

6.6 IGRF Correction

The regional effects of the earth's magnetic field were corrected for by calculating the IGRF value at each fiducial using IGRF model 2010 and secular variation model.

6.7 Diurnal Subtraction

The base station magnetics (diurnal) were filtered using a long wavelength filter to retain wavelengths longer than 51 seconds. This value was subtracted from the IGRF corrected total magnetic intensity and a base value of 48080 nT was added back to the magnetics. This produced the diurnally corrected residual magnetic intensity.

6.8 Tie-line Levelling

At this stage the residual magnetic intensity data were tie-line levelled using Fugro's proprietary ATLAS software.

6.9 Micro-levelling

At this stage the residual magnetic intensity data were micro-levelled using Fugro's proprietary ATLAS software.

6.10 Residual Magnetic Intensity

The residual magnetic intensity data is presented in *Figure 16.*

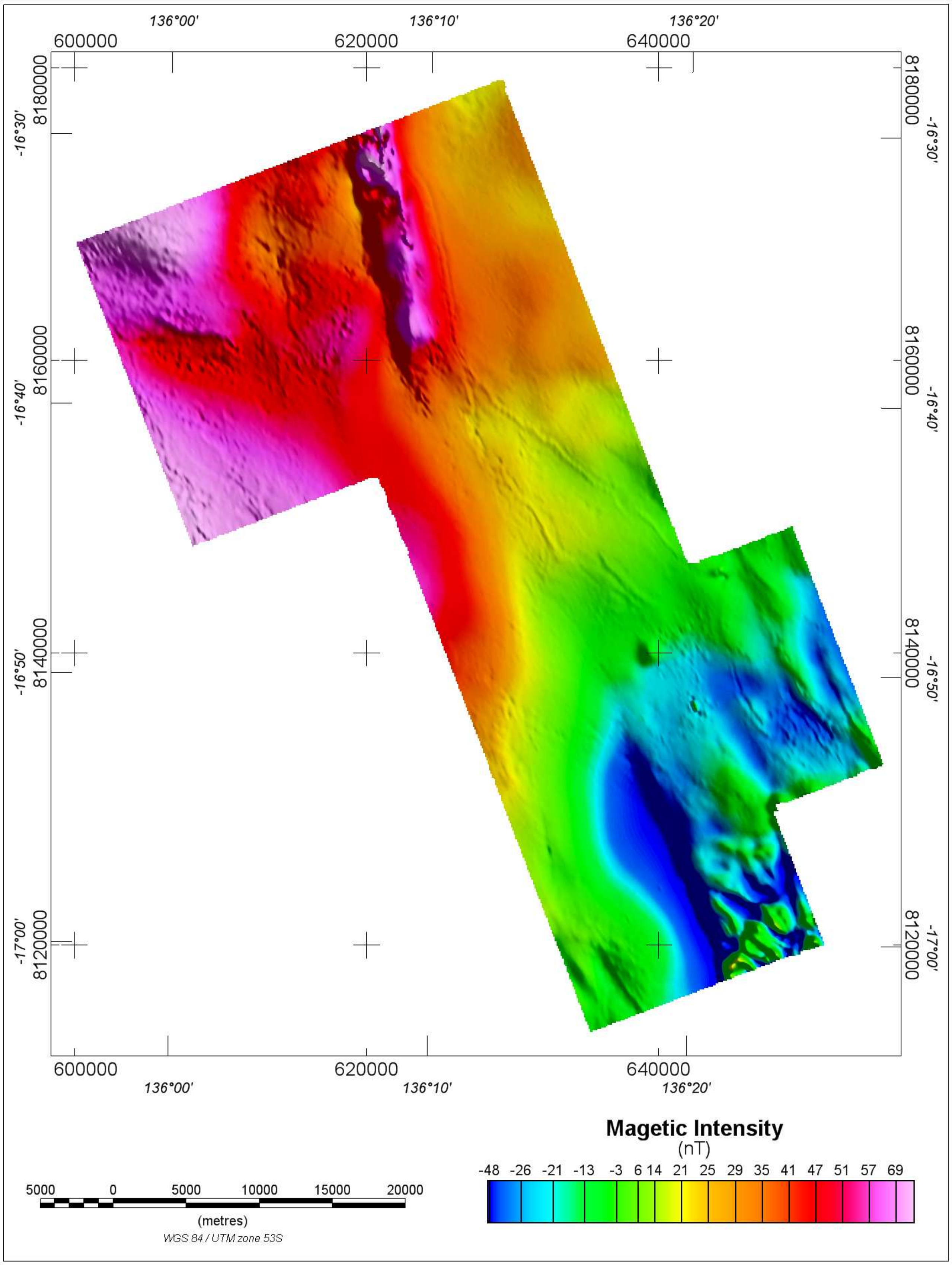

Figure 16: Glyde Sub Basin – *Residual Magnetic Intensity (nT)*

7 APPENDIX I - SURVEY EQUIPMENT

7.1 Survey Aircraft

A Fugro Airborne Surveys Cessna C208B turbo prop, Canadian registration VH-FAY was used to fly the survey area. The following instrumentation was used for this survey.

7.2 FALCON® Airborne Gravity Gradiometer

FALCON® *AGG System* (Cavendish)
The **FALCON®** AGG System is based on current state-of-the-art airborne gravity gradiometer technology and has been optimized for airborne broad band geophysical exploration. The system is capable of supporting surveying activities in areas ranging from 1,000 ft below sea level to 13,000 ft above sea level with aircraft speeds from 70 to 130 knots. The **FALCON®** AGG data streams were digitally recorded at different rates on removable drives installed in the **FALCON®** AGG electronics rack.

7.3 Airborne Data Acquisition Systems

Fugro Digital Acquisition System (FASDAS)
The Fugro FASDAS is a data acquisition system executing propriety software for the acquisition and recording of location, magnetic and ancillary data. Data are presented both numerically and graphically in real time on the VGA display providing on-line quality control capability.

The FASDAS is also used for real time navigation. A pre-programmed flight plan containing boundary coordinates, line start and end coordinates, the altitude values calculated for a theoretical drape surface, line spacing and cross track definitions is loaded into the computer prior to each flight. The WGS-84 latitude and longitude and altitude received from the real-time corrected, dual frequency Novatel OEMV L1/l2-Band Positioning receiver, is transformed to the local coordinate system for cross track and distance to go values. This information, together with ground heading and speed, is displayed to the pilot numerically and graphically on a two line LCD display. It is also presented on the operator LCD screen in conjunction with a pictorial representation of the survey area, survey lines and ongoing flight path.

FALCON® *AGG Data Acquisition System (ADAS)*
The FASDAS provides control and data display for the **FALCON®** AGG system. Data are displayed in real time for the operator and warnings displayed should system parameters deviate from tolerance specifications. All **FALCON®** AGG and laser scanner data are recorded to a removable hard drive.

7.4 Aerial and Ground Magnetometers

The airborne Caesium magnetometer was a Scintrex CS-2 having a noise envelope of 0.002nT pk-pk in 0.01-1Hz bandwidth. The ground magnetometer was a Scintrex CS2 Caesium sensor sampling at 1Hz.

7.5 Real-Time Differential GPS

Novatel OEMV L-Band Positioning
The Novatel OEMV L-band Positioning receiver provides real-time differential GPS for the onboard navigation system. The differential data set was relayed via a geo-synchronous

satellite to the aircraft where the receiver optimized the corrections for the current location.

7.6 GPS Base Station Receiver

Novatel OEM4 L1/L2
The Novatel GPS receiver is a 12 channel dual frequency GPS receiver. It provides raw range information of all satellites in view sampled every second and recorded on a computer laptop. These data are post-processed with the rover data to provide differential GPS (DGPS) corrections for the flight path.

7.7 Altimeters

Collins ALT-55 Radio Altimeter
The radar altimeter has a resolution of 1m, an accuracy of 2%, a range of 1-2,500 ft and a measurement rate of 10 Hz.

7.8 Laser Scanner

Riegl LMS-Q140I-80
The laser scanner is designed for high speed line scanning applications. The system is based upon the principle of time-of-flight measurement of short laser pulses in the infrared wavelength region and the angular deflection of the laser beam is obtained by a rotating polygon mirror wheel. The measurement range is up to 400 m with a minimum range of 2 m and an accuracy of 50mm. The laser beam is eye safe, the laser wavelength is 0.9 µm, the scan angle range is +/- 40º and the scan speed is 20 scans/s.

7.9 Data Processing Hardware and Software

The following equipment and software were used:

Hardware
- One 2.0 GHz (or higher) laptop computer
- External USB hard drive reader for ADAS removable drives
- Two External USB hard drives for data backup
- HP DeskJet All-In-One printer, copier, scanner

Software
- Oasis Montaj data processing and imaging software
- GrafNav Differential GPS processing software
- Fugro - Atlas data processing software
- Fugro - DiAGG processing software

8 APPENDIX II - SYSTEM TESTS

8.1 Instrumentation Lag

Due to the relative position of the magnetometer, altimeters and GPS antenna on the aircraft and to processing/recording time lags, raw readings from each data stream vary in position. To correct for this and to align selected anomaly features on lines flown in opposite directions, the magnetic and altimeter data are ‘parallaxed’ with respect to the position information. The lags were applied to the data during processing.

8.2 Radar Altimeter Calibration

The radar altimeter is checked for accuracy and linearity every 12 months, or when any change in a key system component requires this procedure to be carried out. This calibration allows the radar altimeter data to be compared and assessed with the other height data (GPS, barometric and laser) to confirm the accuracy of the radar altimeter over its operating range. The calibration is performed by flying a number of 30 second lines at preselected terrain clearances over an area of flat terrain and using the results of the radar altimeter, differentially corrected GPS heights in mean sea level (MSL) and laser scanner were used to derive slope and offset information.

8.3 FALCON® AGG Noise Measurement

At the commencement of the survey, 20 minutes of data were collected with the aircraft in straight level flight at 3500 ft AGL. These data were processed as a survey line to check the AGG noise levels.

Daily flight debriefs incorporating **FALCON®** AGG performance statistics for each flight line are prepared using output from Fugro DiAGG software. These are sent daily to Fugro office staff for performance evaluation.

8.4 Daily Calibrations

A set of daily calibrations were performed each survey day as follows:
- Magnetic base station time check
- AGG Quiescent Calibration

8.4.1 Magnetic Base Station Time Check

Prior to each day’s survey all magnetic base stations were synchronised using broadcast GPS time signals.

8.4.2 FALCON® AGG Calibration

A calibration was performed at the beginning of each flight and the results monitored by the operator. The coefficients obtained from each of the calibrations were used in the processing of the data.

9 APPENDIX III - FALCON® AGG DATA & PROCESSING

9.1 Nomenclature

The **FALCON®** airborne gravity gradiometer (AGG) system adopts a North, East, and Down coordinate sign convention and these directions (N, E, and D) are used as subscripts to identify the gravity gradient tensor components (gravity vector derivatives). Lower case is used to identify the components of the gravity field and upper case to identify the gravity gradient tensor components. Thus the parameter usually measured in a normal exploration ground gravity survey is $\mathbf{g_D}$ and the vertical gradient of this component is $\mathbf{G_{DD}}$.

9.2 Units

The vertical component of gravity ($\mathbf{g_D}$) is delivered in the usual units of mGal. The gradient tensor components are delivered in eotvos, which is usually abbreviated to "E". By definition **1 E = $\mathbf{10^{-4}}$ mGal/m.**

9.3 FALCON® Airborne Gravity Gradiometer Surveys

In standard ground gravity surveys, the component measured is "$\mathbf{g_D}$", which is the *vertical component of the acceleration due to gravity*. In airborne gravity systems, since the aircraft is itself accelerating, measurement of "$\mathbf{g_D}$" cannot be made to the same precision and accuracy as on the ground. Airborne gravity gradiometry uses a differential measurement to remove the aircraft motion effects and delivers gravity data of a spatial resolution and sensitivity comparable with ground gravity data.

The **FALCON®** gradiometer instrument acquires two curvature components of the gravity gradient tensor namely $\mathbf{G_{NE}}$ and $\mathbf{G_{UV}}$ where $\mathbf{G_{UV}} = (\mathbf{G_{NN}} – \mathbf{G_{EE}})/2$.

A feature of the **FALCON®** AGG system is that two independent measurements are made of both the NE and UV curvature components. This is achieved by using two sets of accelerometers, referred to as the A complement and the B complement. Each complement consists of four accelerometers. The measured gradients from these complements are referred to as A_{NE} and A_{UV} and B_{NE} and B_{UV}. The $\mathbf{G_{NE}}$ and $\mathbf{G_{UV}}$ gradients are computed by averaging A and B:

$$\mathbf{G_{NE}} = (A_{NE} + B_{NE})/2$$
$$\mathbf{G_{UV}} = (A_{UV} + B_{UV})/2$$

Since these curvature components cannot easily and intuitively be related to the causative geology, they are transformed into the vertical gravity gradient ($\mathbf{G_{DD}}$), and integrated to derive the vertical component of gravity ($\mathbf{g_D}$). Interpreters display, interpret and model both $\mathbf{G_{DD}}$ and $\mathbf{g_D}$. The directly measured $\mathbf{G_{NE}}$ and $\mathbf{G_{UV}}$ data are appropriate for use in inversion software to generate density models of the earth. The vertical gravity gradient, $\mathbf{G_{DD}}$, is more sensitive to small or shallow sources and has greater spatial resolution than $\mathbf{g_D}$ (similar to the way that the vertical magnetic gradient provides greater spatial resolution and increased sensitivity to shallow sources of the magnetic field). In the integration of $\mathbf{G_{DD}}$ to give $\mathbf{g_D}$, the very long wavelength component, at wavelengths comparable to or greater than the size of the survey area, cannot be fully recovered. Long wavelength gravity are therefore incorporated in the $\mathbf{g_D}$ data from other sources. This might be regional ground, airborne or marine gravity if such data are available. The Danish National Space Centre global gravity data of 2008 (DNSC08) are used as a default if other data are not available.

9.4 Gravity Data Processing

The main elements and sequence of processing of the gravity data are given below. Unless not applicable or specified otherwise, the processing step is applied to each individual complement element (A_{NE}, A_{UV}, B_{NE}, B_{UV}):

1. Dynamic corrections for residual aircraft motion (called Post Mission Compensation or PMC) are calculated and applied.
2. Self gradient corrections are calculated and applied to reduce the time-varying gradient response from the aircraft and platform.
3. A Digital Terrain Model (DTM) is created from the laser scanner range data, the AGG inertial navigation system rotation data and the DGPS position data.
4. Terrain corrections are calculated and applied.
5. Tie line levelling, and micro-levelling (where necessary) are applied.
6. $\mathbf{G_{NE}}$ and $\mathbf{G_{UV}}$ are transformed into the full gravity gradient tensor, including $\mathbf{G_{DD}}$, and into $\mathbf{g_D}$.

9.5 Aircraft dynamic corrections

The design and operation of the **FALCON®** AGG results in very considerable reduction of the effects of aircraft acceleration but residual levels are still significant and further reduction is required and must be done in post-processing.

Post-processing correction relies on monitoring the inertial acceleration environment of the gravity gradiometer instrument (GGI) and constructing a model of the response of the GGI to this environment. Parameters of the model are adjusted by regression to match the sensitivity of the GGI during data acquisition. The modelled GGI output in response to the inertial sensitivities is subtracted from the observed output. Application of this technique to the output of the GGI, when it is adequately compensated by its internal mechanisms, reduces the effect of aircraft motion to acceptable levels.

Following these corrections, the gradient data are demodulated and filtered along line using a 6-pole Butterworth low-pass filter with a cut-off frequency of 0.18 Hz.

9.6 Self gradient Corrections

The GGI is mounted in gimbals controlled by an inertial navigation system which keeps the GGI pointing in a fixed direction whilst the aircraft and gimbals rotate around it. Consequently, the GGI measures a time-varying gravity gradient due to these masses moving around it as the heading and attitude of the aircraft changes during flight. This is called the self-gradient.

Like the aircraft dynamic corrections, the self-gradient is calculated by regression of model parameters against measured data. In this case, the rotations of the gimbals are the input variables of the model. Once calculated, the modelled output is subtracted from the observed output.

9.7 Laser Scanner Processing

The laser scanner measures the range from the aircraft to the ground in a swath of angular width ±40 degrees below the aircraft. The aircraft attitude (roll, pitch and heading) data provided by the AGG inertial navigation system are used to adjust the range data for changes in attitude and the processed differential GPS data are used to reference the range data to located ground elevations referenced to the WGS 84 datum. Statistical filtering strategies are used to remove anomalous elevations due to foliage or built up environment. The resulting elevations are gridded to form a digital terrain model (DTM).

9.8 Terrain Corrections

An observation point above a hill has excess mass beneath it compared to an observation point above a valley. Since gravity is directly proportional to the product of the masses, uncorrected gravity data have a high correlation with topography.

It is therefore necessary to apply a terrain correction to gravity survey data. For airborne gravity gradiometry at low survey heights, a detailed DTM is required. Typically, immediately below the aircraft, the digital terrain will need to be sampled at a cell size roughly one-third to one-half of the survey height and with a position accuracy of better than 1 metre. For these accuracies, LIDAR data are required and each **FALCON®** survey aircraft comes equipped with LIDAR (laser scanner).

If bathymetric data are used then these form a separate terrain model for which terrain corrections are calculated at a density chosen to suit the water bottom – water interface. Once the DTM has been merged, the terrain corrections for each of the $\mathbf{G_{NE}}$ and $\mathbf{G_{UV}}$ data streams are calculated. In the calculation of terrain corrections, a density of 1 gm/cc is used. The calculated corrections are stored in the database allowing the use of any desired terrain correction density by subtracting the product of desired density and correction from the measured $\mathbf{G_{NE}}$ and $\mathbf{G_{UV}}$ data. The terrain correction density is chosen to be representative of the terrain density over the survey area. Sometimes more than one density is used with input from the client.

Typically, the terrain corrections are calculated over a distance 10 km from each survey measurement point.

9.9 Tie line Levelling

The terrain- and Self gradient-corrected $\mathbf{G_{NE}}$ and $\mathbf{G_{UV}}$ data are tie line levelled across the entire survey using a least-squares minimisation of differences at survey line intersections. Occasionally some micro-levelling might be performed.

9.10 Transformation into G_{DD} & g_D

The transformation of the measured, corrected and levelled $\mathbf{G_{NE}}$ and $\mathbf{G_{UV}}$ data into gravity and components of the full gravity gradient tensor is accomplished using two methods:

- Fourier domain transformation and
- Equivalent source transformation.

The input data for the Fourier method are the average **NE** and **UV** components computed from the complement data, as described in section *9.3*. The Fourier method relies on the Fourier transform of Laplace's equation. The application of this transform to the complex function $\mathbf{G_{NE} + i\, G_{UV}}$ provides a stable and accurate calculation of each of the full tensor components and gravity. The Fourier method performs piece-wise upward and downward continuation to work with data collected on a surface that varies from a flat horizontal plane. For stability of the downward continuation, the data are low-pass filtered. The cut-off wavelength of this filter depends on the variations in altitude and the line spacing. It is set to the smallest value that provides stable downward continuation.

In survey areas where the variability of the terrain surface (and hence the flight surface) makes it impossible to obtain Fourier transformation results that are both high resolution and stable, an alternate method can be applied which bypasses the upward and downward continuation steps. The results are calculated at the flight surface. This approach lacks the mathematical rigour of the complete method but allows for greater detail in the output data.

The input data for the equivalent source method are the individual **NE** and **UV** component data from each complement, as referred to in section **Error! Reference source not found.**. The equivalent source method relies on a smooth model inversion to calculate the density of a surface of sources and from these sources, a forward calculation provides the $\mathbf{G_{DD}}$ and $\mathbf{g_D}$ data. The smoothing results in an output that is equivalent to the result of the low-pass filter in the Fourier domain method.

The Fourier method generates all tensor components but the equivalent source method only generates $\mathbf{G_{DD}}$ and $\mathbf{g_D}$ (and $\mathbf{G_{NE}}$ and $\mathbf{G_{UV}}$ for comparison with the inputs).

The limitations of gravity gradiometry in reconstructing the long wavelengths of gravity can lead to differences in the results of these two methods at long wavelength. The merging of the $\mathbf{g_D}$ data with externally supplied regional gravity such as the DNSC08 gravity provides a way of reducing these differences.

9.11 Terrain Corrections Using Alternate Terrain Densities

Although both uncorrected processed and transformed data and unit density terrain correction data are supplied, it is not recommended that these be used to create final data corrected for any arbitrary terrain correction density. The principal reason for this is that tie line levelling occurs after application of the terrain correction. As a result, levelling errors present in the terrain correction channels by virtue of positional inaccuracy are not removed from these channels and will be present in any data corrected with them. Further, filtering applied in creating the uncorrected, transformed data is not applied to the terrain correction channels. Mixing data filtered in different ways is not advised.

An alternative method uses the linear relationship between the terrain corrections at different densities and the corresponding gravity gradient or $\mathbf{g_D}$ values. This method can be applied to either the grid data or the located data. An example is given using $\mathbf{G_{DD}}$:

The new density is referred to as ρ_N, the existing densities as ρ_1 and ρ_2

$$\mathbf{G_{DD}}(\rho_N) = \mathbf{G_{DD}}(\rho_1) + (\mathbf{G_{DD}}(\rho_2) - \mathbf{G_{DD}}(\rho_1))*(\rho_N - \rho_1)/(\rho_2 - \rho_1)$$

Note that the terrain correction channel is eliminated by substitution in deriving this equation.

It is recommended that two densities that differ by a reasonable value be used for this method, in order to minimise uncertainties caused by noise in the data. The values of 0.00 and 2.67 g/cm^3 usually delivered should be sufficient to yield useful results.

9.12 Noise & Signal

By taking two independent measurements of the NE and UV curvature components at each sample point, it is possible to obtain a direct indication of the reliability of these measurements. The standard deviation of half the difference of the pairs of measurements - (A_{NE},B_{NE}) and (A_{UV},B_{UV}) - provides a good estimate of the survey noise:

$$Noise_{NE} = StdDev((A_{NE} - B_{NE})/2)$$
$$Noise_{uv} = StdDev((A_{uv} - B_{uv})/2)$$

These difference channels are calculated for each data point. The standard deviation across all data points is the figure quoted for the survey as a whole.

This difference error has been demonstrated to follow a 'normal' or Gaussian statistical distribution, with a mean of zero. Therefore, the bulk of the population (95%) will lie between -2σ and +2σ of the mean. For a typical survey noise estimate of, say, 3 E, 95% of the noise will be between -6 E and +6 E.

These typical errors in the curvature gradients translate to errors in $\mathbf{G_{DD}}$ of about 5 E and in $\mathbf{g_D}$ (in the shorter wavelengths) in the order of 0.1 mGal.

9.13 Risk Criteria in Interpretation

The risks associated with a **FALCON®** AGG survey are mainly controlled by the following factors.

- **Survey edge anomalies** – the transformation from measured curvature gradients to vertical gradient and vertical gravity gradient is subject to edge effects. Hence any anomalies located within about 2 x line spacing of the edge of the survey boundaries should be treated with caution.

- **Single line anomalies** – for a wide-spaced survey, an anomaly may be present on only one line. Although it might be a genuine anomaly, the interpreter should note that no two-dimensional control can be applied.

- **Low amplitude (less than 2σ) anomalies** – Are within the noise envelope and need to be treated with caution, if they are single line anomalies and close in diameter to the cut-off wavelengths used.

- **Residual topographic error anomalies** – Inaccurate topographic correction either due to inaccurate DTM or local terrain density variations may produce anomalies. Comparing the DTM with the G_{DD} map terrain-corrected for different densities is a reliable way to confirm the legitimacy of an anomaly.

- **The low density of water and lake sediments** – (if present) can create significant gravity and gravity gradient lows which may be unrelated to bedrock geology. It is recommended that all anomalies located within lakes or under water be treated with caution and assessed with bathymetry if available.

9.14 References

Boggs, D. B. and Dransfield, M. H., 2004, Analysis of errors in gravity derived from the Falcon® airborne gravity gradiometer, Lane, R. (ed.), Airborne Gravity 2004 - Abstracts from the ASEG-PESA Airborne Gravity 2004 Workshop, Geoscience Australia Record 2004/18, 135-141.

Dransfield, M. H., 2010, Conforming Falcon gravity and the global gravity anomaly, Geophysical Prospecting, 58, 469-483.

Dransfield, M. H. and Lee, J. B., 2004, The FALCON® airborne gravity gradiometer survey systems, Lane, R. (ed.), Airborne Gravity 2004 - Abstracts from the ASEG-PESA Airborne Gravity 2004 Workshop, Geoscience Australia Record 2004/18, 15-19.

Dransfield, M. H. and Zeng, Y., Airborne gravity gradiometry: terrain corrections and elevation error, *submitted to Geophysics*.

Lee, J. B., 2001, FALCON Gravity Gradiometer Technology, Exploration Geophysics, 32, 75-79.

Lee, J. B.; Liu, G.; Rose, M.; Dransfield, M.; Mahanta, A.; Christensen, A. and Stone, P., 2001, High resolution gravity surveys from a fixed wing aircraft, Geoscience and Remote Sensing Symposium, 2001. IGARSS '01. IEEE 2001 International, 3, 1327-1331.

Stone, P. M. and Simsky, A., 2001, Constructing high resolution DEMs from Airborne Laser Scanner Data, Preview, Extended Abstracts: ASEG 15th Geophysical Conference and Exhibition, August 2001, Brisbane, 93, 99.

10 APPENDIX IV - FINAL PRODUCTS

Final **FALCON®** AGG digital line data were provided in 8 Hz ASCII and Geosoft Oasis GDB database files containing the fields and format described in *Table 2* below.

Final aeromagnetic digital line data were provided in 10Hz ASCII and Geosoft Oasis GDB database files containing the fields and format described in *Table 3* below.

Grids of Fourier and equivalent source products, Total Magnetic Intensity, as well as the DTM were delivered, as described in *Table 4* below. The grids are in ERMapper ERS formats with a 100 m cell size, with the exception of the DTM grid which has a 25 m cell size.

One copy of the digital archives was delivered along with a hard copy of this Logistics and Processing Report.

Field	Variable	Description	Units
1	EASTING	WGS84 UTM53S Easting	metres
2	NORTHING	WGS84 UTM53S Northing	metres
3	Line	Line number	
4	Flight	Flight number	
5	Date	Gregorian Date	YYYYMMDD
6	LONGITUDE	WGS84 Longitude	degrees
7	LATITUDE	WGS84 Latitude	degrees
8	ALTITUDE_Ellipsoid	GPS antenna height above WGS84 ellipsoid	metres
9	ALTITUDE	GPS antenna height above WGS84 ellipsoid with geoid (EGM96) correction applied	metres
10	time	Universal Time (seconds since January 6 1980)	seconds
11	alt_RADAR	Radar altimeter (aircraft's height above terrain as measured by the radar altimeter)	metres
12	HEIGHT	Flying height, (aircraft's height above terrain as derived from laser scanner and ALTITUDE data)	metres
13	DTM	Terrain height above WGS84 ellipsoid with Geoid (EGM96) correction applied	metres
14	TURBULENCE	Estimated vertical platform turbulence (vertical acceleration where g = 9.80665 m/sec/sec)	milli g
15	T_DD	Terrain effect calculated for DD using a density of 1g/cc	eotvos
16	T_NE	Terrain effect calculated for NE using a density of 1g/cc	eotvos
17	T_UV	Terrain effect calculated for UV using a density of 1g/cc	eotvos
18	Err_NE	NE gradient uncorrelated noise estimate, after levelling	eotvos
19	Err_UV	UV gradient uncorrelated noise estimate, after levelling	eotvos
20	A_NE_2p67	Self gradient, jitter & terrain corrected NE gradient, terrain correction density 2.67 g/cc	eotvos
21	A_UV_2p67	Self gradient, jitter & terrain corrected UV gradient, terrain correction density 2.67 g/cc	eotvos
22	B_NE_2p67	Self gradient, jitter & terrain corrected NE gradient, terrain correction density 2.67 g/cc	eotvos
23	B_UV_2p67	Self gradient, jitter & terrain corrected UV gradient, terrain correction density 2.67 g/cc	eotvos
24	A_NE_0	Self gradient & jitter corrected NE gradient, no terrain correction applied	eotvos
25	A_UV_0	Self gradient & jitter corrected UV gradient, no terrain correction applied	eotvos

26	B_NE_0	Self gradient & jitter corrected NE gradient, no terrain correction applied	eotvos
27	B_UV_0	Self gradient & jitter corrected UV gradient, no terrain correction applied	eotvos
28	gD_FOURIER_2p67	Fourier derived vertical Gravity, terrain correction density 2.67 g/cc, 400 m cut-off wavelength	mGal
29	GDD_FOURIER_2p67	Fourier derived vertical gravity gradient, terrain correction density 2.67 g/cc, 400 m cut-off wavelength	eotvos
30	GEE_FOURIER_2p67	Fourier derived Gee gradient, terrain correction density 2.67 g/cc, 400 m cut-off wavelength	eotvos
31	GNN_FOURIER_2p67	Fourier derived Gnn gradient, terrain correction density 2.67 g/cc, 400 m cut-off wavelength	eotvos
32	GED_FOURIER_2p67	Fourier derived Ged horizontal EW gradient, terrain correction density 2.67 g/cc, 400 m cut-off wavelength	eotvos
33	GND_FOURIER_2p67	Fourier derived Gnd horizontal NS gradient, terrain correction density 2.67 g/cc, 400 m cut-off wavelength	eotvos
34	GNE_FOURIER_2p67	Fourier derived Gne curvature gradient, terrain correction density 2.67 g/cc, 400 m cut-off wavelength	eotvos
35	GUV_FOURIER_2p67	Fourier derived Guv curvature gradient, terrain correction density 2.67 g/cc, 400 m cut-off wavelength	eotvos
36	gD_FOURIER_0	Fourier derived vertical Gravity, no terrain correction applied, 400 m cut-off wavelength	mGal
37	GDD_FOURIER_0	Fourier derived vertical gravity gradient, no terrain correction applied, 400 m cut-off wavelength	eotvos
38	GEE_FOURIER_0	Fourier derived Gee gradient, no terrain correction applied, 400 m cut-off wavelength	eotvos
39	GNN_FOURIER_0	Fourier derived Gnn gradient, no terrain correction applied, 400 m cut-off wavelength	eotvos
40	GED_FOURIER_0	Fourier derived Ged horizontal EW gradient, no terrain correction applied, 400 m cut-off wavelength	eotvos
41	GND_FOURIER_0	Fourier derived Gnd horizontal NS gradient, no terrain correction applied, 400 m cut-off wavelength	eotvos
42	GNE_FOURIER_0	Fourier derived Gne curvature gradient, no terrain correction applied, 400 m cut-off wavelength	eotvos
43	GUV_FOURIER_0	Fourier derived Guv curvature gradient, no terrain correction applied, 400 m cut-off wavelength	eotvos
44	DRAPESURFACE_FOURIER	Drape surface for Fourier reconstruction, smoothed flight surface	metres
45	gD_EQUIV_2p67	Equivalent source derived vertical gravity, terrain correction density 2.67 g/cc - source depth 400 m	mGal
46	GDD_EQUIV_2p67	Equivalent source derived vertical gravity gradient, terrain correction density 2.67 g/cc - source depth 400 m	eotvos
47	GNE_EQUIV_2p67	Equivalent source derived Gne curvature gradient, terrain correction density 2.67 g/cc - source depth 400 m	eotvos
48	GUV_EQUIV_2p67	Equivalent source derived Guv curvature gradient, terrain correction density 2.67 g/cc - source depth 400 m	eotvos
49	gD_EQUIV_0	Equivalent source derived vertical gravity, no terrain correction applied - source depth 400 m	mGal
50	GDD_EQUIV_0	Equivalent source derived vertical gravity gradient, no terrain correction applied - source depth 400 m	eotvos
51	GNE_EQUIV_0	Equivalent source derived Gne curvature gradient, no terrain correction applied - source depth 400 m	eotvos
52	GUV_EQUIV_0	Equivalent source derived Guv curvature gradient, no terrain correction applied - source depth 400 m	eotvos
53	DRAPESURFACE_EQUIV	Drape surface for equivalent source reconstruction, smoothed flight surface	metres
54	LEVMAG	Final levelled magnetics	nT

Table 2: Final FALCON® AGG Digital Data – *ASCII and Geosoft Database Format*

Field	Variable	Description	Units
1	EASTING	WGS84 UTM53S Easting	metres
2	NORTHING	WGS84 UTM53S Northing	metres
3	Line	Line number	
4	Flight	Flight number	
5	Date	Gregorian Date	YYYYMMDD
6	LONGITUDE	WGS84 Longitude	degrees
7	LATITUDE	WGS84 Latitude	degrees
8	ALTITUDE_Ellipsoid	GPS antenna height above WGS84 ellipsoid	metres
9	ALTITUDE	GPS antenna height above WGS84 ellipsoid with geoid (EGM96) correction applied	metres
10	time	Universal Time (seconds since January 6 1980)	seconds
11	alt_RADAR	Radar altimeter (aircraft's height above terrain as measured by the radar altimeter)	metres
12	DTM	Terrain height above WGS84 ellipsoid with Geoid (EGM96) correction applied (sampled from DTM grid)	metres
13	RAWMAG	Raw magnetic intensity - Lagged, unfiltered, uncompensated TMI	nT
14	COMPMAG	Compensated magnetic intensity - Lagged, de-spiked, compensated TMI	nT
15	DIURNAL	Despiked, lightly filtered ground station mag	nT
16	IGRF	IGRF TMI based on date, location and altitude of each point (IGRF model 2010)	nT
17	DCMAG	COMPMAG after subtraction of the IGRF and DIURNAL	nT
18	LEVMAG	DCMAG after tie line levelling and micro-levelling	nT
19	FLUX_X	Fluxgate X component	nT
20	FLUX_Y	Fluxgate Y component	nT
21	FLUX_Z	Fluxgate Z component	nT

Table 3: Final Aeromagnetic Digital Data – *ASCII and Geosoft Database Format*

File	Description	Units
2349_1_mag_final	Total Magnetic Intensity	nT
2349_1_DTM_final	Terrain (Referenced to EGM96 geoid)	metres
2349_1_equiv_drape_surface_final	Drape surface for equivalent source computation, 85 m above terrain	metres
2349_1_equiv_gD_2p67_final	Equivalent source derived vertical gravity, terrain correction density 2.67 g/cm^3	mGal
2349_1_equiv_gD_2p67_conformed_final	Equivalent source derived vertical gravity, terrain correction density 2.67 g/cm^3 conformed to regional gravity	mGal
2349_1_equiv_GDD_2p67_final	Equivalent source derived vertical gravity gradient, terrain correction density 2.67 g/cm^3	eotvos
2349_1_equiv_gD_0_final	Equivalent source derived vertical gravity, no terrain correction applied	mGal
2349_1_equiv_gD_0_conformed_final	Equivalent source derived vertical gravity, no terrain correction applied conformed to regional gravity	mGal
2349_1_equiv_GDD_0_final	Equivalent source derived vertical gravity gradient, no terrain correction applied	eotvos
2349_1_Fourier_drape_surface_final	Drape surface for Fourier computation, smoothed flight surface	metres
2349_1_Fourier_gD_2p67_final	Fourier derived vertical gravity, terrain correction density 2.67 g/cm^3	mGal
2349_1_Fourier_gD_2p67_conformed_final	Fourier derived vertical gravity, terrain correction density 2.67 g/cm^3 conformed to regional gravity	mGal
2349_1_Fourier_GDD_2p67_final	Fourier derived vertical gravity gradient, terrain correction density 2.67 g/cm	eotvos
2349_1_Fourier_gD_0_final	Fourier derived vertical gravity, no terrain correction applied	mGal
2349_1_Fourier_gD_0_conformed_final	Fourier derived vertical gravity, no terrain correction applied conformed to regional gravity	mGal
2349_1_Fourier_GDD_0_final	Fourier derived vertical gravity gradient, no terrain correction applied	eotvos

Table 4: Final Aeromagnetic and AGG Grids – *ERMapper Format*